Bioorganic Chemistry 92 (2019) 103236

Contents lists available at ScienceDirect

Bioorganic Chemistry

journal homepage: www.elsevier.com/locate/bioorg

Dual-targeting antitumor conjugates derived from platinum(IV) prodrugs and microtubule inhibitor CA-4 significantly exhibited potent ability to overcome cisplatin resistance

Xiaochao Huang[a,*,1], Meng Wang[a,1], Chungu Wang[b], Weiwei Hu[a], Qinghong You[a], Yong Yang[a], Chunhao Yu[a], Zhixin Liao[b], Shaohua Gou[b,*], Hengshan Wang[c,*]

[a] Jiangsu Key Laboratory of Regional Resource Exploitation and Medicinal Research, Huaiyin Institute of Technology, Huaian 223003, China
[b] Jiangsu Province Hi-Tech Key Laboratory for Biomedical Research, Southeast University, Nanjing 211189, China
[c] State Key Laboratory for the Chemistry and Molecular Engineering of Medicinal Resources, School of Chemistry and Pharmaceutical Sciences of Guangxi Normal University, Guilin 541004, China

ARTICLE INFO

Keywords:
Platinum(IV) prodrugs
Antitumor activity
CA-4
Apoptosis

ABSTRACT

Here we report that three platinum(IV) prodrugs containing a tubulin inhibitor CA-4, as dual-targeting platinum (IV) prodrug, were synthesized and evaluated for antitumor activity using MTT assay. Among them, complex **9** exhibited the most potent antitumor activity against the tested cancer lines including cisplatin resistance cancer cells, and simultaneously displayed lower toxicity compared to cisplatin, respectively. Moreover, complex **9**, in which was conjugated to an inhibitor of tubulin at one axial position of platinum(IV) complex, could effectively enter the cancer cells, and significantly induce cell apoptosis and arrest the cell cycle in A549 cells at G2/M stage, and dramatically disrupt the microtubule organization. In addition, mechanism studies suggested that complex **9** significantly induced reactive oxygen species (ROS) generation and decreased mitochondrial transmembrane potential (MMP) in A549 cells, and effectively induced activation of caspases triggering apoptotic signaling through mitochondrial dependent apoptosis pathways.

1. Introduction

Since the introduction of platinum(II)-based drug cisplatin into the clinic about 40 years ago, cisplatin and its analogues (Fig. 1), such as carboplatin and oxaliplatin have become the most widely used for the treatment of numerous types of cancer [1–4]. However, drug resistance is one of the most important issues to hamper its chemotherapeutic efficacy in solid tumors in addition to the well-known serious side effects of these platinum(II)-based complexes [5–7]. Therefore, various strategies aimed at discovering new platinum(II) drugs with at least equal activity as well as low toxicity compared to cisplatin have been conducted [8]. Unfortunately, only a little of platinum(II) drugs entered clinical trials and most of them failed. In order to search for more effective platinum drugs to overcome these drawbacks of platinum(II) chemotherapeutics, platinum(IV) complexes have shown great promise [9–12]. Platinum(IV) complex is kinetically more inert compared to platinum(II) complexes, and it is widely accepted that they used as prodrugs, which can be activated by intracellular reduction and reduced to platinum(II) equivalents following cellular uptake [11,12]. In recently years, some research studies suggested that platinum(IV) complexes conjugated biologically active moieties in the axial position could effectively improve the antitumor activities in addition to overcome the side effect of platinum(II) drugs (Fig. 2) [13–16].

In recently, some studies also suggested that single drug chemotherapy usually suffered from poor therapeutic efficacy, severe drug resistance and adverse side effects after frequent administration owing to the complexity and heterogeneity of various solid tumors [17–19]. Therefore, combination chemotherapy, which uses two or multiple drugs with different target sites and mechanisms of action, has been regarded as an important strategy to overcome the limitations of single drug chemotherapy. The chemotherapeutic agent combretastatin A-4 (CA-4, **4**, Fig. 3) and its derivatives, such as combretastatin A-4-phosphate (Fig. 3) and serine amino acid analogue of CA-4 (AVE8062, Fig. 3), which could strongly inhibit tubulin polymerization through combining the colchicine binding site, were found to exhibit excellent anticancer activities against many types of solid tumors including

* Corresponding authors.
E-mail addresses: viphuangxc@126.com (X. Huang), sgou@seu.edu.cn (S. Gou), whengshan@163.com (H. Wang).
[1] Co-first author: These authors contributed equally to this work.

https://doi.org/10.1016/j.bioorg.2019.103236
Received 11 July 2019; Received in revised form 21 August 2019; Accepted 30 August 2019
Available online 30 August 2019

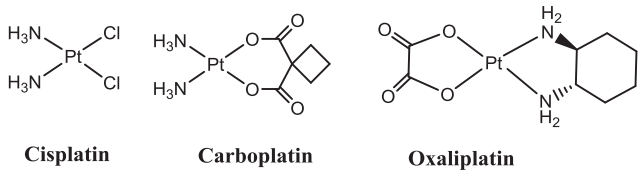

Fig. 1. FDA approved Pt(II) anticancer agents.

multidrug resistant cancer cell lines [20–24]. Moreover importantly, CA-4 and its analogues are currently under clinical trials as a single drug or in combination for anticancer therapy [25–27]. Thus, it can be imagined that the combination of platinum anticancer agents with tubulin inhibitor CA-4 could effectively improve therapeutic profiles and overcome the side effect of platinum(II) agents.

Aiming at this goal, according to the unique structural features and reactive inertness of platinum(IV) complexes, three tubulin-targeting platinum(IV) prodrugs were synthesized and prepared as shown in Scheme 1. In the present study, we characterized these platinum(IV) complexes and evaluated their *in vitro* anticancer activities as well as their mechanism of action. The results of mechanistic experiments revealed that complex **9** could effectively induce cell apoptosis, elevate the ROS level of cancerous lung cells and inhibit cell migration and invasion *in vitro*, respectively. Furthermore, our study further demonstrated that the potent anticancer activity of complex **9** was related to tubulin inhibition, DNA damage, and activation of the mitochondrial signaling pathway.

2. Results and discussion

2.1. Design and synthesis

The synthetic route to prepare platinum(IV) complexes **9–11** are shown in Scheme 1. Firstly, the natural product CA-4 and compound **1** were obtained according to the former methods [28,29]. Secondly, compound **5** was achieved by the formation of ester bond between **4** and glutaric anhydride in the presence of potassium carbonate in DMF. The synthesis of three platinum(IV) complexes **6**, **7** and **8** were prepared through the oxidative chlorination of the corresponding platinum (II) complexes with N-chlorosuccinimide (NCS) in water according to the reported procedure. [30] Finally, the title complexes **9–11** were obtained by esterification between **5** and **6**, **7** or **8** in the presence of TBTU/Et_3N in DMF. Meanwhile, the resulting title complexes **9–11** were characterized by ^1H NMR, ^{13}C NMR spectra and elemental analysis together with ESI-MS spectroscopy.

2.2. In vitro cytotoxicity

The *in vitro* cytotoxicity of complexes **9–11** were investigated using MTT assays on four human cancer cell lines, SK-OV-3 (ovarian), HepG-2 (hepatocellular), MGC-803 (gastric), NCI-H460 (lung) and human normal liver cells HL-7702, using cisplatin, oxaliplatin, DACHPt and CA-4 as the positive drug controls, respectively. The cytotoxicities were expressed as IC_{50} values presented in Table 1. The results listed in Table 1 indicated that CA-4 displayed excellent antitumor activities toward four human cancer cell lines as expected. Interestingly, platinum (IV) complexes **9–11**, which were attached to an inhibitor of tubulin at one axial position of platinum(IV) complexes octahedral coordination sphere, possessed higher activity than their corresponding platinum(II) complexes (cisplatin, DACHPt and oxaliplatin). Especially, complex **9**, the platinum (IV) derivative of cisplatin with one CA-4 ligand in the axial position, gave the IC_{50} values of 0.17–0.20 μM toward four cancer cell lines, which displayed a 29.2–34.2 fold increase in activity compared to cisplatin, respectively. Moreover, complex 9 synchronously showed lower cytotoxicity toward human normal liver HL-7702 cells with IC_{50} values of 12.67 ± 1.15 than that of cisplatin (11.81 ± 1.11) and CA-4 (6.21 ± 1.05), respectively. More importantly, the selectivity index of complex **9** was calculated out as 70.4, much higher than that of cisplatin (2.2) and CA-4 (29.5). The similar results were also observed in complexes **10** and **11**. Taken together, the *in vitro* evaluation results suggesting that three platinum (IV) complexes displayed lower cytotoxicity than their corresponding platinum(II) complexes against human normal liver cells HL-7702, suggesting that these complexes have a selective toxicity for the tumor cells over the normal cell.

2.3. Antitumor activity of complex 9 against cisplatin resistant cancer cells

Drug resistance is a key therapeutic problem that demonstrated the efficacies of cisplatin for different solid tumors, such as human lung cancer cells A549 [5,6]. Therefore, it is important to develop new antiproliferative agents against drug-resistant cancer cell lines. In present study, we further evaluated the cytotoxicity of complex **9** against cisplatin sensitive and resistant cancer cells (A549 and A549/CDDP). The cytotoxicities were expressed as IC_{50} values presented in Table 2. The results listed in Table 2 indicated that the IC_{50} value of cisplatin against A549/CDDP resistant cells was increased to 21.56 μM, while, complex **9** was not obviously changed for the cisplatin resistant cancer cells compared to cisplatin sensitive cells, with IC_{50} values of 0.13 ± 0.03 μM and 0.16 ± 0.05 μM toward this pair of cancer cells, respectively. It was much significant to discover that complex **9** had a low resistance factors (1.13) compared with cisplatin (5.07). In short, the results listed in Table 2 indicated that complex **9** nearly equally potent activity against cisplatin-resistant A549 cells might be useful in the treatment of drug refractory cancer resistance to cisplatin.

2.4. Complex 9 induced apoptosis in A549 cells

In order to confirm whether cell apoptosis was induced by complex **9** in the A549 cells, cells were stained with Annexin V-FITC as an apoptosis marker and PI as a cell viability marker. Thus, in this study, A549 cells were treated with complex **9** and cisplatin at the indicated concentrations for 24 h, and the percentages of apoptotic cells were determined by flow cytometry, respectively. As shown in Fig. 4, after treatment with 5.0 or 10 μM of **9** for 24 h, the percentage of apoptosis cells was enhanced from 17.42 to 27.64%, while that of control was only 2.70%. Notably, the apoptosis of A549 cells treatment with the compound increased gradually in a dose-dependent manner. More importantly, the 27.64% induction of A549 cell apoptosis with incubation with 10 μM of **9** was significantly higher than that of cisplatin (12.76% apoptotic cells at the same concentration). On the basis of these results, complex **9** could significantly induce apoptosis in A549 cells at the indicated concentrations.

2.5. Cellular uptake

Since complex **9** exhibited the most potent antitumor activity against the tested cancer cell lines, thus, it was selected to carry out the cellular uptake test in A549 cells by using the inductively coupled plasma mass spectrometry (ICP-MS). As shown in Table 3, treating A549 cells with **9** (5.0 and 10 μM) for 12 h resulted in a substantial enhance in the content of cellular platinum in a concentration-dependent manner, indicating facile internalization of complex **9** within 24 h. Notably, the uptake of complex **9** was remarkably higher than those of cisplatin at the indicated concentration. After A549 cells exposure to 10 μM with **9** for 24 h, the concentration of cellular platinum increase to 362 ng/10^6 cells, which was nearly up to 1.86 times as much as that of cisplatin (10 μM). Thus, the outcomes of this experimental seem to indicate that the improvement of cellular uptake could result in improved therapeutic profiles.

The experiments were performed three times, and the results of the representative experiments are shown.

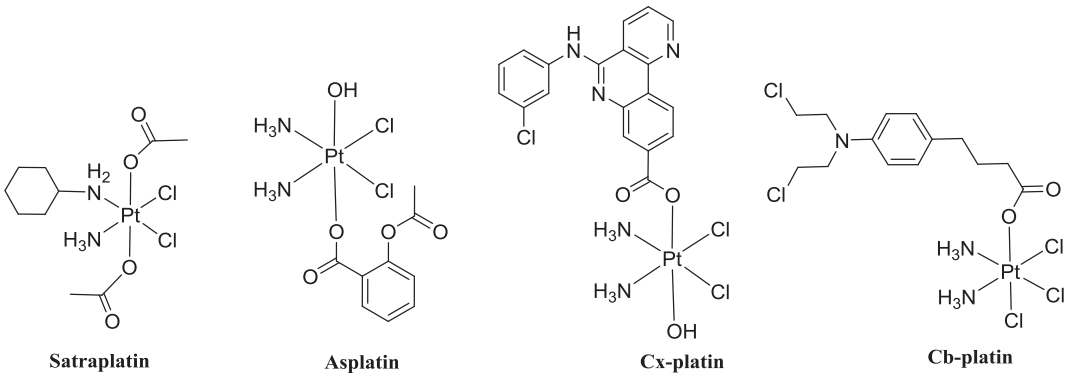

Fig. 2. Chemical structures of a few platinum(IV) prodrugs.

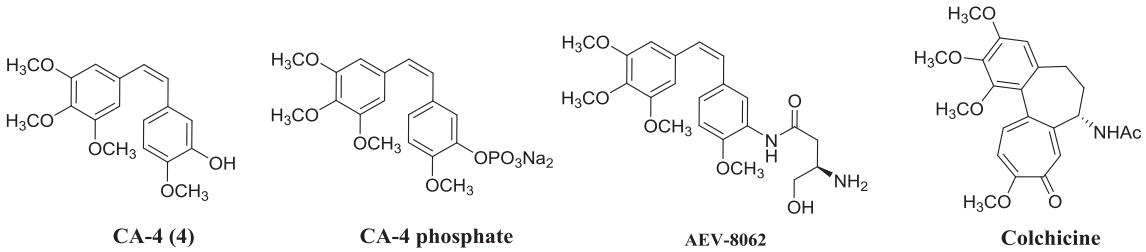

Fig. 3. Structures of natural products and clinical trial agents.

2.6. Cell cycle analysis

In order to explore if the cytotoxicity of complex **9** was due to the cell cycle arrest, therefore, we investigated the effect on cell cycle progression using PI-staining by flow cytometry analysis in A549 cells. As shown in Fig. 5, complex **9** induced cell cycle arrest at the G2/M stage in a dose-dependent manner. Notably, the percentage of cells in the G2/M phase were 23.18% and 36.61% when the cells were treated with complex **9** for 24 h at the indicated concentrations of 5 and 10 μM, respectively (Fig. 5). In control (untreated cells) 11.46% of accumulation in G2/M phase was observed, while the percentage of cells in the G2/M phase only increased to 14.95% after treatment with cisplatin at 10 μM for 24 h. In shorts, the outcomes of cell cycle experimental suggested that complex **9** markedly arrested the G2/M phase of the cell cycle in a concentration-dependent manner.

2.7. Complex *9* inhibited the migration of A549 cells in vitro

Recently, some of studies reported that the metastatic tumor cells displayed great capability of migration and invasion [31,32]. Meanwhile, migration is a key step in the process of tumor metastasis. Thus, a well-established wound-healing assay was conducted to examine if complex **9** could prevent the migration of A549 cells. As shown in Fig. 6A, the wounds of A549 cells without drug treatment showed 66.3% closure after 24 h, in contrast, the wounds of cells showed 51.4% closure after treatment with cisplatin at 10 μM, respectively. Interestingly, the wounds of A549 cells exhibited 33.8% and 18.4% after incubation with 5 and 10 μM of complex **9** for 24 h, respectively (Fig. 6A). Moreover, for evaluation of cell invasion, transwell migration assays were conducted to further examine whether complex **9** could prevent the migration of human lung cancer A549 cells. As shown in Fig. 6B, the presence of complex **9** effectively weakened the migration of A549 cells in a concentration-dependent manner. In shorts, these results indicated that complex **9** remarkably attenuated the migration of A549 cells in a concentration-dependent manner.

2.8. Analysis of immunofluorescence staining

Owing to tubulin-microtubule system plays an important role in the maintenance of cell shape and basic cellular functions [33,34], here an immunofluorescence assay was performed to investigate if complex **9** could disrupt the microtubule dynamics in human lung cancer A549 cells. In present study, we investigated the effect on the cellular microtubule network treated with 5 and 10 μM of complex **9** for 24 h, and stained for α-tubulin (green) and DNA (blue). As shown in Fig. 7, in the control groups, the microtubule network in the A549 cells exhibited normal arrangement and organization, characterized by regularly assembled in the absence of drug treatment. As expected, as shown in Fig. 7, cells treatment with 5 μM of CA-4 exhibited dramatically disrupted microtubule organization. Notably, cells after exposure to complex **9** at 5 and 10 μM for 24 h, the spindle formation demonstrated distinct abnormalities and showed heavily disrupted microtubule organization (Fig. 7), respectively. These morphological microtubules changes suggested that complex **9** remarkably disrupted the microtubule organization caused the multipolarization of the mitotic spindle, and interfered with the mitosis of A549 at the indicated concentrations, indicating that tubulin is an effective target for its anticancer activity.

2.9. Complex *9* triggered mitochondrial pathway dependent apoptosis

Many studies indicated that the mitochondria participate in the induction of apoptosis, and loss of mitochondrial trans-membrane potential (MMP) is an early event in apoptotic process [35–37]. In addition, increasing evidences revealed that the triggering of various death pathways including intrinsic and extrinsic begins with the dysfunction of mitochondria. Thus, in order to explore the contribution of mitochondria in complex **9** induced cell apoptosis, we examined MMP, which is measurably affected under conditions of mitochondrial dysfunction using JC-1 staining by flow cytometry analysis in A549 cells. The untreated A549 cells were used as negative control. The A549 cells were incubated with complex **9** and cisplatin at the same concentration for 24 h, respectively. As shown in Fig. 8, it was worth noted that after cells exposed to complex **9** from 5 to 10 μM, the red fluorescence intensity decreased from 83.26% to 74.2% compared to control group,

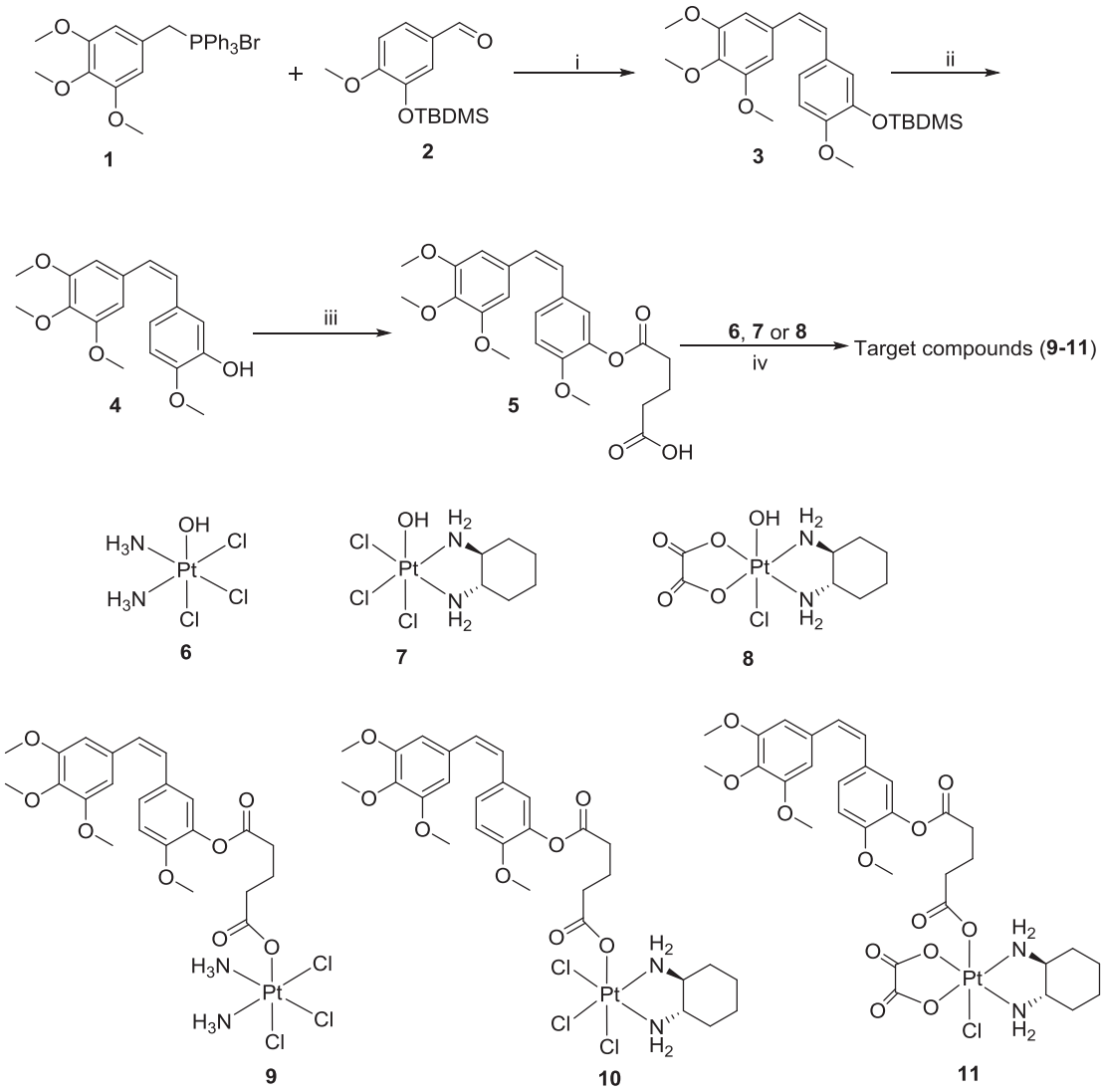

Scheme 1. Synthetic pathway to target complexes **9–11**. Reagents and conditions: (i) NaH, CH_2Cl_2, room temperature, overnight; (ii) p-toluenesulfonic acid, CH_3OH, 50 °C, overnight; (iii) Glutaric anhydride, K_2CO_3, DMF (N,N-Dimethylformamide), room temperature, 2 h; (iv) TBTU, Et_3N, DMF, 30 °C, overnight.

respectively. Notably, it was observed that complex **9** was remarkably caused mitochondrial dysfunction in human lung cancer A549 cells than that of cisplatin. In shorts, these results clearly demonstrated that complex **9** remarkably caused MMP collapse and mitochondrial dysfunction, and eventually induced cell apoptosis in A549 cells.

2.10. Complex 9 triggered ROS generation

In the past years, many studies indicated that compromised mitochondria could effectively cause an increase in ROS levels, which can in turn alter cell function or induce apoptosis [38,39]. In addition,

Table 1
Cytotoxic effects of complexes **9–11** on human cancer and normal cell lines.

Compds.	IC_{50} (μM)[d]					
	Sk-OV-3	HepG-2	MGC-803	NCI-H460	HL-7702	SI[e]
9	0.19 ± 0.08	0.18 ± 0.07	0.20 ± 0.06	0.17 ± 0.13	12.67 ± 1.15	70.4
10	0.21 ± 0.11	0.25 ± 0.13	0.19 ± 0.12	0.23 ± 0.14	11.33 ± 1.87	45.3
11	0.20 ± 0.09	0.34 ± 0.10	0.28 ± 0.11	0.31 ± 0.11	14.08 ± 1.65	41.4
CA-4	0.23 ± 0.10	0.21 ± 0.08	0.29 ± 0.13	0.18 ± 0.08	6.21 ± 1.05	29.5
CDDP[a]	6.05 ± 1.28	5.26 ± 1.09	6.81 ± 1.13	5.82 ± 1.03	11.81 ± 1.91	2.2
DACHPt[b]	5.35 ± 1.34	8.63 ± 1.22	4.59 ± 1.54	5.28 ± 1.19	10.52 ± 1.44	1.2
Oxa[c]	10.07 ± 1.43	9.18 ± 1.16	7.24 ± 1.54	9.83 ± 1.37	13.66 ± 1.68	1.5

[a] Cisplatin.
[b] Dichloro(1R,2R-diaminocyclohexane)platinum(II).
[c] Oxaliplatin.
[d] In vitro cytotoxicity was determined by MTT assay upon incubation of the live cells with the compounds for 72 h.
[e] Selectivity Index = IC_{50}(HL-7702)/IC_{50}(HepG-2). Mean values based on three independent experiments.

Table 2
Biological activity of tested compounds against cisplatin sensitive and resistant cancer cells (A549 and A549/CDDP).

Comp.	IC_{50} (μM)[b]		
	A549	A549/CDDP	Resistant factor
9	0.15 ± 0.03	0.17 ± 0.05	1.13
CA-4	0.21 ± 0.09	0.32 ± 0.12	1.52
CDDP[a]	4.25 ± 1.06	21.56 ± 1.93	5.07

[a] Cisplatin.
[b] In vitro cytotoxicity was determined by MTT assay upon incubation of the live cells with the compounds for 72 h. Mean values based on three independent experiments, and the results of the representative experiments are shown.

Table 3
Cellular uptake of complex **9** in A549 cells.

Complex	Pt content (ng/10^6 cells)
	A549
9 (5 μM)	163 ± 17
9 (10 μM)	362 ± 38
Cisplatin (5 μM)	103 ± 13
Cisplatin (10 μM)	195 ± 21

many studies have demonstrated that the death-inducing capacity of chemotherapeutic drugs has been associated with the production of ROS [40,41]. Therefore, we further investigated if ROS stimulated by complex **9** induced apoptosis in A549 cells. Cells were treated with complex **9** (5 and 10 μM) for 24 h using 2′, 7′-dichlorofluorescein diacetate (DCFH-DA) staining analysis by flow cytometry. As shown in Fig. 9, after exposure to 2.5 μM of complex **9** for 24 h, the production of ROS level was increased to 29.41% compared to control group (1.06%). Interestingly, when the concentration of complex **9** was increased to 10 μM, the production of ROS level was increased to 48.21%, which was more than three times that of cisplatin (14.85% under the same concentration), respectively. The results suggested that the Pt(IV) complex **9** induced the production of significant amounts of ROS, which could ultimately in turn lead to A549 cells apoptosis.

*2.11. Complex **9** induced apoptosis via the activation of caspases and regulated apoptosis-related protein expression*

To further provide more mechanistic insight into how complex **9** induces apoptosis, we examined the expression of apoptotic proteins Bax, Bcl-2, caspases (caspase-3 and -9) and PARP in response to complex **9** treatment. Thus, A549 lung cancer cells were treated with or without complex **9** for 24 h by means of western blotting, and GAPDH

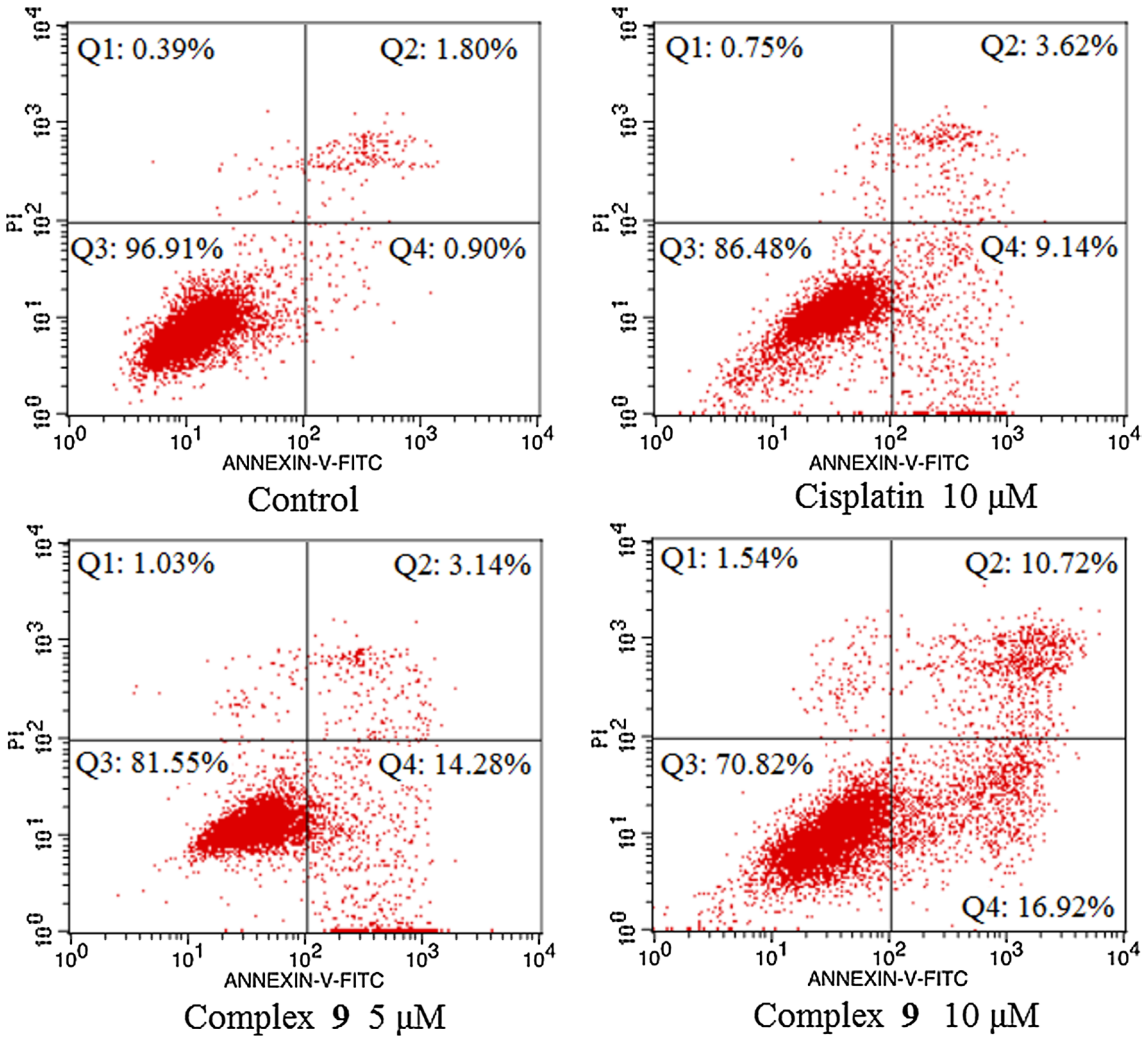

Fig. 4. Representative flow cytometric histograms of apoptotic A549 cells after 24 h treatment with complex **9** (5, 10 μM) and cisplatin (10 μM) as positive control. The cells were harvested and labeled with annexin-V-FITC and PI, and analyzed by flow cytometry. Q1, Q2, Q3, and Q4 represent four different cell states: necrotic cells, late apoptotic or necrotic cells, living cells and apoptotic cells, respectively. Data are expressed as the mean ± SEM for three independent experiments.

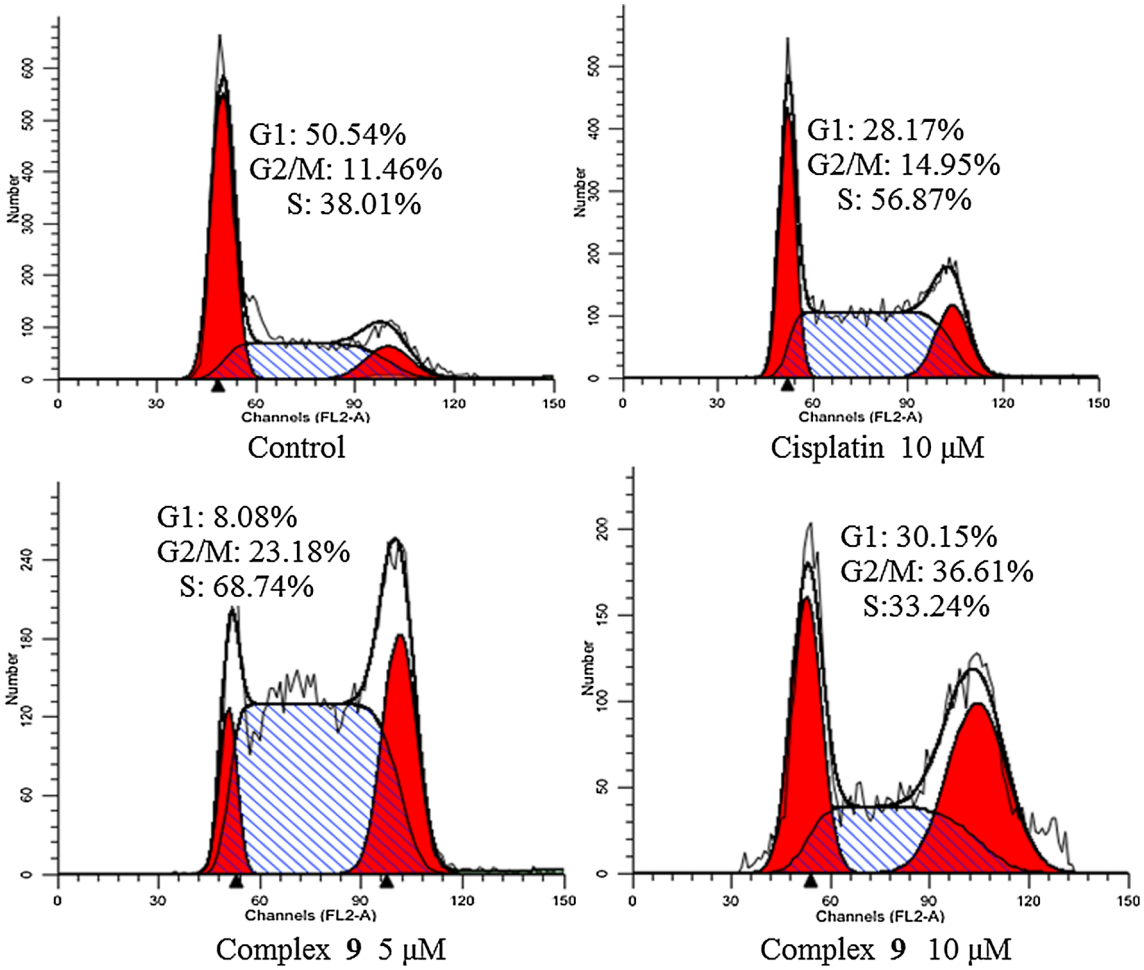

Fig. 5. Cell cycle arrest effect of complex **9**. A549 cells treated with complex **9** and cisplatin at the indicated concentrations for 24 h. Then, the cells were trypsinized, harvested and washed three times with ice-PBS for PI-stained DNA content detected by flow cytometry.

expression was served as an internal control groups. As indicated in Fig. 10, complex **9** remarkably enhanced the expression levels of the pro-apoptosis proteins Bax, but suppressed the levels of pro-survival protein Bcl-2 expression in a dose-dependent manner. Moreover, complex **9** resulted in more significant expression of caspase-3 and -9 and PARP compared to the cisplatin-treated group, respectively (Fig. 10). Taken together, these results have further demonstrated that complex **9** treatment induced apoptosis in A549 cells.

3. Conclusions

In summary, according to the unique structural features and reactive inertness of platinum(IV) complexes, three tubulin-targeting platinum(IV) prodrugs were successfully designed, synthesized and evaluated for antitumor activity. Firstly, results of cytotoxicity experiments *in vitro* revealed that these three platinum(IV) complexes not only exhibited greater potency in anti-proliferative activity than that of their mother platinum(II) counterparts against tested cancer cell lines including cisplatin resistant cancer cells, but also showed less toxic compared to their corresponding platinum(II) complexes against human normal liver HL-7702, respectively. Notably, complex **9**, the platinum(IV) derivative of cisplatin with one CA-4 ligand in the axial position, possessed better anti-proliferative activities against tested cancer cell lines (SK-OV-3, HepG-2, MGC-803 and NIC-H460) than the FDA-approved clinical chemotherapeutic agent cisplatin, with IC_{50} values in the range of 0.17–0.20 μM, which exhibited a 29.2–34.2 fold increase in activity compared to cisplatin, respectively. Furthermore, the anticancer activity of complex **9** was not obviously changed for the cisplatin resistant A549/CDDP cells than that of the cisplatin sensitive A549 cells. Secondly, complex **9** effectively induced cell apoptosis, caused cell cycle arrest at G2/M phase and heavily disrupted the microtubule organization. In addition, treatment of A549 cells with complex **9** demonstrated a significant inhibition of cell migration and invasion *in vitro*. Finally, our studies demonstrated that complex **9** induced apoptotic cell death of A549 cells via a mitochondrial mediated pathway by production of reactive oxygen species (ROS), down-regulating Bcl-2 and up-regulating Bax, which in turn lead to activate downstream caspase-9 and -3. These results are consistent with the apoptosis induced by chemotherapeutics of intrinsic pathways, and additional biological evaluations are ongoing in our lab and the results will be reported in due course.

4. Experimental section

All chemicals and solvents were analytical reagent grade and commercially available, and used without further purification unless noted specifically. Column chromatography was performed using silica gel (200–400 mesh). Mass spectra were measured on an Agilent 6224 TOF LC/MS instrument. Elemental analyses of C, H, and N used a Vario MICRO CHNOS elemental analyzer (Elementary). ^{1}H NMR and ^{13}C NMR spectra were recorded in $CDCl_3$ or DMSO-d_6 with a Bruker 500 MHz NMR spectrometer.

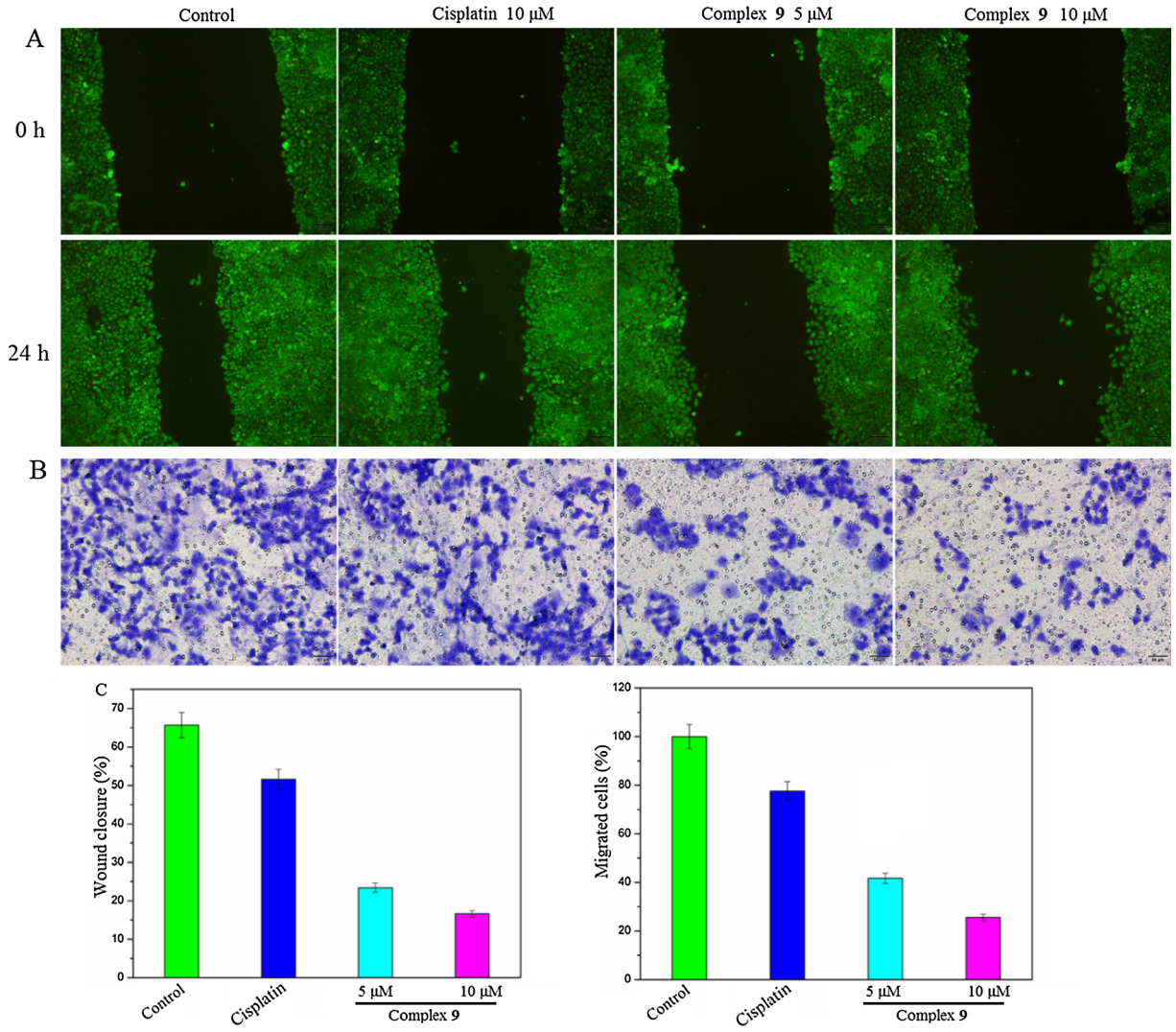

Fig. 6. (A) Migration inhibition (wound-healing assay) of A549 cells treated without or with the tested complex **9** and cisplatin for 24 h at the indicated concentrations. Typical images were taken at 0 and 24 h. (B) Cell invasion of A549 cells after incubation with the tested complex **9** and cisplatin at the indicated concentrations for 24 h by transwell assay. The widths of wounds are indicated with the lines (mm). (C) Quantification of confocal images. Widths are statistically significant with $P < 0.05$.

*4.1. General procedure for the preparation of complexes **9–11***

Synthesis of compound **3.** To a solution of compounds **1** (12.0 g, 22.99 mmol) in dry dichloromethane (100 mL) was cooled to ice-water and added NaH (3.8 g, 95.8 mmol). The reaction mixture was stirred for 30 min at the same temperature. Then compound **2** (5.1 g, 19.16 mmol) in dry dichloromethane (20 mL) was added dropwise to the reaction. The mixture reaction was stirred at room temperature for overnight, and monitored by TLC using ethyl acetate and petroleum ether. After completion of the reaction, the reaction mixture was quenched with ice water and washed with water (200 mL). The combined organic phases were washed with brine solution, dried over anhydrous Na_2SO_4 and evaporated under vacuum to afford crude product. The residue was purified on a silica gel column eluted with petroleum ether/ethyl acetate to give the desired product **3** (3.2 g, yield 38.9%) as yellow oil. ^{1}H NMR (500 MHz, $CDCl_3$) δ 6.85 (d, J = 8.3 Hz, 1H), 6.79 (d, J = 2.1 Hz, 1H), 6.73 (d, J = 8.3 Hz, 1H), 6.50 (s, 2H), 6.47 (d, J = 12.1 Hz, 1H), 6.42 (d, J = 12.1 Hz, 1H), 3.83 (s, 3H), 3.78 (s, 3H), 3.70 (s, 6H), 0.93 (s, 9H), 0.06 (s, 6H). HR-MS (m/z) (ESI): calcd for $C_{24}H_{35}O_5Si$ $[M+H]^+$: 431.2254; found: 431.2246.

Synthesis of compound **4.** To a solution of compound **3** (3.1 g, 7.2 mmol) and in dry MeOH (20 mL), $TsOH{\cdot}H_2O$ (684 mg, 3.6 mmol) was added and the reaction was stirred at room temperature for overnight and monitored by TLC using ethyl acetate and petroleum ether. After completion of reaction, the solvent was removed under vacuum, and the resulting residue was diluted with water (200 mL) and extracted with CH_2Cl_2 (2 × 100 mL). The combined organic phases was dried over anhydrous Na_2SO_4 and concentrated under vacuum. The residue was purified on a silica gel column eluted with petroleum ether/ethyl acetate to obtain the target product (2.1 g, yield 91.3%) as a white solid. ^{1}H NMR (500 MHz, $CDCl_3$) δ 6.92 (d, J = 1.9 Hz, 1H), 6.79 (d, J = 8.3 Hz, 1H), 6.73 (d, J = 8.3 Hz, 1H), 6.52 (s, 2H), 6.46 (d, J = 12.2 Hz, 1H), 6.40 (d, J = 12.2 Hz, 1H), 5.58 (s, 1H), 3.85 (s, 3H), 3.84 (s, 3H), 3.69 (s, 6H). HR-MS (m/z) (ESI): calcd for $C_{18}H_{21}O_5$ $[M+H]^+$: 317.1389; found: 317.1379.

Synthesis of compound **5.** To a solution of compound **4** (1.5 g, 4.7 mmol) and anhydrous K_2CO_3 (1.3 g, 9.4 mmol) in dry DMF (10 mL), glutaric anhydride (1.6 g, 14.1 mmol) was added in reaction, and the reaction was stirred at 50 °C for 2 h and monitored by TLC. After completion of reaction, the mixture was adjusted to pH = 2–3 with 1 N HCl solution, and then the mixture was added CH_2Cl_2 (200 mL), washed with water (3 × 200 mL). The combined organic layer was dried over anhydrous Na_2SO_4 and concentrated under vacuum. The residue was purified on a silica gel column eluted with methanol/dichloromethane

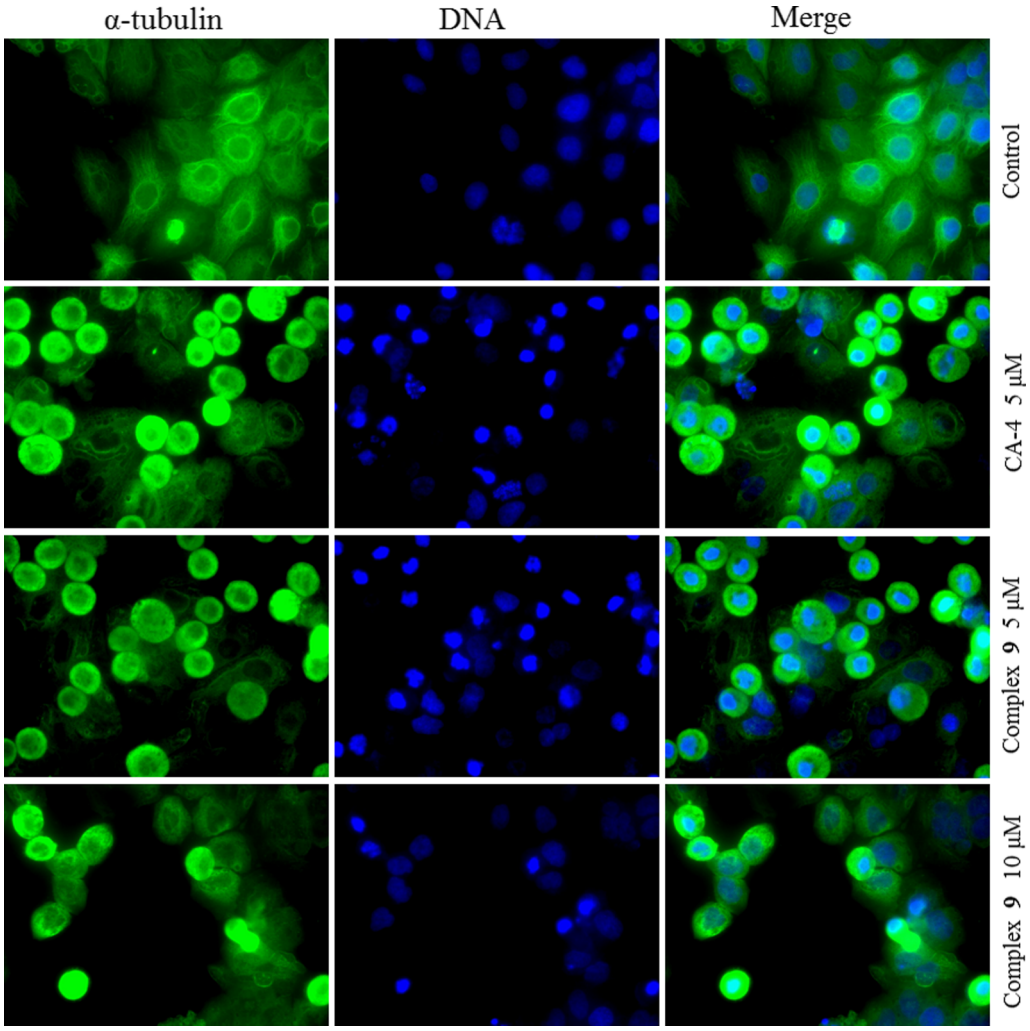

Fig. 7. Effects of complex **9** on the microtubule network of cells. Untreated cells were served as negative control and cells treated with 5 and 10 μM of complex **9** for 24 h were fixed in methanol and stained with α-tubulin and counterstained with 4, 6-diamidino-2-phenylindole (DAPI). CA-4 was served as positive drug. Microtubules and unassembled tubulin are shown in red. DNA, stained with DAPI, is shown in blue. Data are expressed as the mean ± SEM of three independent experiments.

to obtain the desired product **5** (1.1 g, yield 55.0%) as a white solid. ^{1}H NMR (500 MHz, DMSO-d_6) δ 12.12 (s, 1H), 7.15 (d, J = 8.5 Hz, 1H), 7.07 (d, J = 8.5 Hz, 1H), 6.99 (d, J = 1.8 Hz, 1H), 6.54 (s, 2H), 6.51 (d, J = 12.2 Hz, 1H), 6.48 (d, J = 12.2 Hz, 1H), 3.75 (s, 3H), 3.64 (s, 3H), 3.61 (s, 6H), 2.56 (t, J = 7.3 Hz, 2H), 2.32 (t, J = 7.3 Hz, 2H), 1.83–1.79 (m, 2H). HR-MS (m/z) (ESI): calcd for $C_{23}H_{26}O_5Na$ [M + Na]$^+$: 453.1525; found: 453.1536.

Synthesis of compounds **9–11.** To a solution of compound **5** (150 mg, 0.35 mmol), TBTU (168 mg, 0.53 mmol), and Et_3N (54 mg, 0.53 mmol) in dry DMF (3 mL), complex **6**, **7** or **11** (0.35 mmol) was added. The mixture was stirred at 30 °C for overnight and monitored by TLC. After completion of reaction, the mixture reaction was added to dichloromethane (200 mL), and then extracted twice with water (200 mL). The organic phase was dried over anhydrous Na_2SO_4 and concentrated under reduced pressure. The residue was purified on silica gel column eluted methanol/dichloromethane to obtain the desired product **9**, **10** or **11**.

Compound **9**. 120 mg, 44.9% yield as a yellow solid. ^{1}H NMR (500 MHz, DMSO-d_6) δ 7.14 (d, J = 8.5 Hz, 1H), 7.06 (d, J = 8.5 Hz, 1H), 6.98 (d, J = 2.0 Hz, 1H), 6.54 (s, 2H), 6.48 (d, J = 12.2 Hz, 1H), 6.46 (d, J = 12.2 Hz, 1H), 6.39–5.96 (m, 6H), 3.75 (s, 3H), 3.64 (s, 3H), 3.60 (s, 6H), 2.58 (t, J = 7.3 Hz, 2H), 2.35 (t, J = 7.3 Hz, 2H), 1.83–1.75 (m, 2H). ^{13}C NMR (125 MHz, DMSO-d_6) δ 180.22, 171.51, 153.10, 150.54, 139.55, 137.29, 132.44, 130.00, 129.86, 128.77, 127.76, 123.17, 113.16, 106.44, 60.57, 56.43, 56.07, 35.50, 33.00, 21.42. Elemental analysis calcd (%) for $C_{23}H_{31}Cl_3N_2O_8Pt$: C, 36.11; H, 4.09; N, 3.66; found: C, 36.28; H, 4.24; N, 3.41. HR-MS (m/z) (ESI): calcd for $C_{23}H_{32}Cl_3N_2O_8Pt$ [M + H]$^+$: 764.0872; found: 764.0853.

Compound **10**. 135 mg, 45.8% yield as a yellow solid. ^{1}H NMR (500 MHz, DMSO-d_6) δ 9.58–9.53 (t, J = 9.3 Hz, 1H), 8.19–8.09 (m, 1H), 7.97–7.73 (m, 1H), 7.50– 7.38 (m, 1H), 7.14 (d, J = 8.4 Hz, 1H), 7.06 (d, J = 8.4 Hz, 1H), 6.98 (d, J = 2.0 Hz, 1H), 6.54 (s, 2H), 6.48 (d, J = 12.2 Hz, 1H), 6.46 (d, J = 12.2 Hz, 1H), 3.75 (s, 3H), 3.64 (s, 3H), 3.60 (s, 6H), 2.69 (s, 1H), 2.58 (t, J = 7.3 Hz, 2H), 2.36 (t, J = 13.0 Hz, 2H), 2.19 (d, J = 10.5 Hz, 1H), 2.06 (d, J = 11.6 Hz, 1H), 1.85–1.80 (m, 2H), 1.58–1.48 (m, 3H), 1.33–1.23 (m, 2H), 1.15–1.02 (m, 2H). ^{13}C NMR (125 MHz, DMSO-d_6) δ 182.91, 171.34, 153.10, 150.51, 139.55, 137.31, 132.43, 130.02, 129.87, 128.76, 127.75, 123.19, 113.17, 106.45, 63.89, 62.70, 60.56, 56.43, 56.07, 36.67, 32.86, 31.40, 31.32, 24.07, 24.03, 21.45. Elemental analysis calcd (%) for $C_{29}H_{39}Cl_3N_2O_8Pt$: C, 41.22; H, 4.65; N, 3.31; found: C, 41.38; H, 4.78; N, 3.08. HR-MS (m/z) (ESI): calcd for $C_{29}H_{39}Cl_3N_2O_8PtNa$ [M + Na]$^+$: 866.1317; found: 866.1337.

Compound **11**. 165 mg, 53.4% yield as a yellow solid. ^{1}H NMR (500 MHz, DMSO-d_6) δ 8.40–8.26 (m, 3H), 7.67–7.63 (m, 1H), 7.14 (d, J = 8.5 Hz, 1H), 7.06 (d, J = 8.5 Hz, 1H), 6.98 (d, J = 1.8 Hz, 1H), 6.53

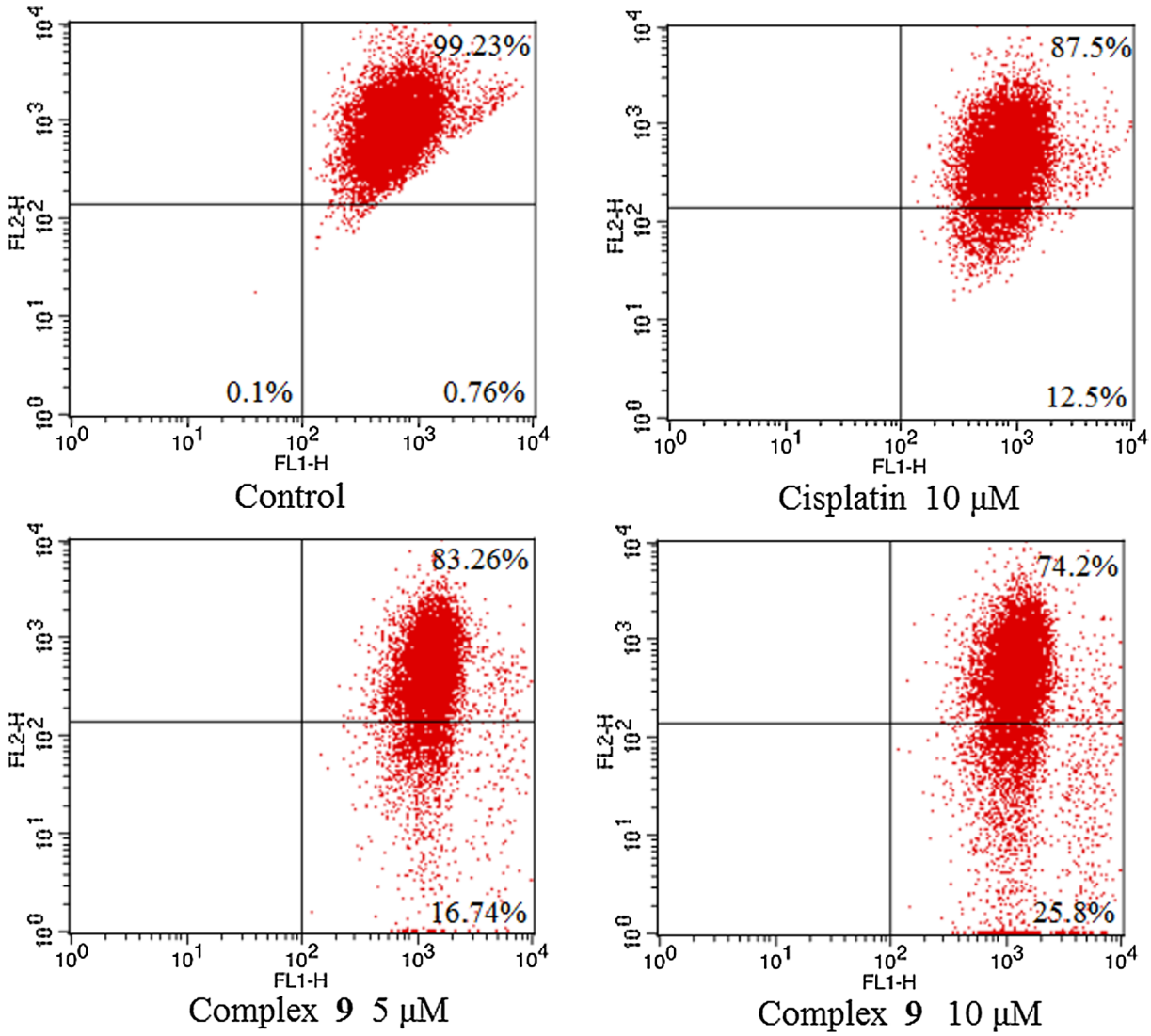

Fig. 8. Complex **9** decreased the MMP of A549 cells. The A549 cells were treated with **9** and cisplatin at the indicated concentrations for 24 h followed by incubation with the fluorescence probe JC-1 for 30 min. Then, the cells were analyzed by flow cytometry. The experiments were performed three times, and the results of the representative experiments are shown.

(s, 2H), 6.48 (d, J = 12.2 Hz, 1H), 6.47 (d, J = 12.2 Hz, 1H), 3.73 (s, 3H), 3.64 (s, 3H), 3.60 (s, 6H), 2.63 (d, J = 24.0 Hz, 1H), 2.58 (t, J = 7.3 Hz, 2H), 2.39 (t, J = 7.3 Hz, 2H), 2.10 (d, J = 10.6 Hz, 1H), 2.02 (d, J = 11.8 Hz, 1H), 1.82–1.75 (m, 2H), 1.58–1.36 (m, 3H), 1.15–1.06 (m, 4H). ^{13}C NMR (125 MHz, DMSO-d_6) δ 180.51, 171.25, 163.67, 153.10, 150.49, 139.52, 137.31, 132.43, 130.03, 129.88, 128.75, 127.76, 123.18, 113.15, 106.44, 61.98, 61.89, 60.55, 56.36, 56.06, 35.84, 32.88, 31.39, 31.06, 24.16, 24.00, 21.28. Elemental analysis calcd (%) for $C_{31}H_{39}ClN_2O_{12}Pt$: C, 43.19; H, 4.56; N, 3.25; found: C, 43.39; H, 4.69; N, 3.03. HR-MS (m/z) (ESI): calcd for $C_{31}H_{39}ClN_2O_{12}PtNa$ $[M+H]^+$: 884.1737; found: 884.1745.

4.2. In vitro cytotoxicity

In this study, all human cancer cell lines (SK-OV-3, HepG-2, MGC-803, A549 and A549/CDDP) and human normal cells (HL-7702) were purchased from the Shanghai Cell Bank of the Chinese Academy of Sciences. Culture medium Roswell Park Memorial Institute (RPMI-1640), phosphate buffered saline (PBS, pH = 7.2), fetal bovine serum (FBS), and Antibiotice-Antimycotic came from KeyGen Biotech Company (China). All cancer cell lines were cultivate in the supplemented with 10% FBS, and human normal liver HL-7702 cells were cultivate in the supplemented with 10% FBS, 100 units/ml of penicillin and 100 g/ml of streptomycin in a humidified atmosphere of 5% CO_2 at 37 °C. Tested compounds were dissolved to stock concentrations of 2 mM with DMF (Sigma); however, cisplatin (Sigma) used as a positive control was directly dissolved in saline, and the cytotoxicity of all complexes against the tested cancer cell lines and human normal cancer cells was evaluated by MTT assay. All data were independently tested repeated in triplicate.

4.3. Cell uptake

A549 cells were seeded in each well of 24-well plates. After the cells reached about 80% confluence, 5.0 and 10 μM of complex **9** and cisplatin were added and the plates were also incubated for 24 h at the same conditions. After completion of 24 h incubation, cells were collected and washed thrice in PBS, then centrifuged at 1000g for 10 min and re-suspended in 2 mL PBS. A volume of 0.1 mL was taken out to detect the cell density, and the remaining A549 cells were digested by HNO_3 (200 μL, 65%) at 65 °C for 12 h, and then the Pt level in cells were examined by ICP-MS.

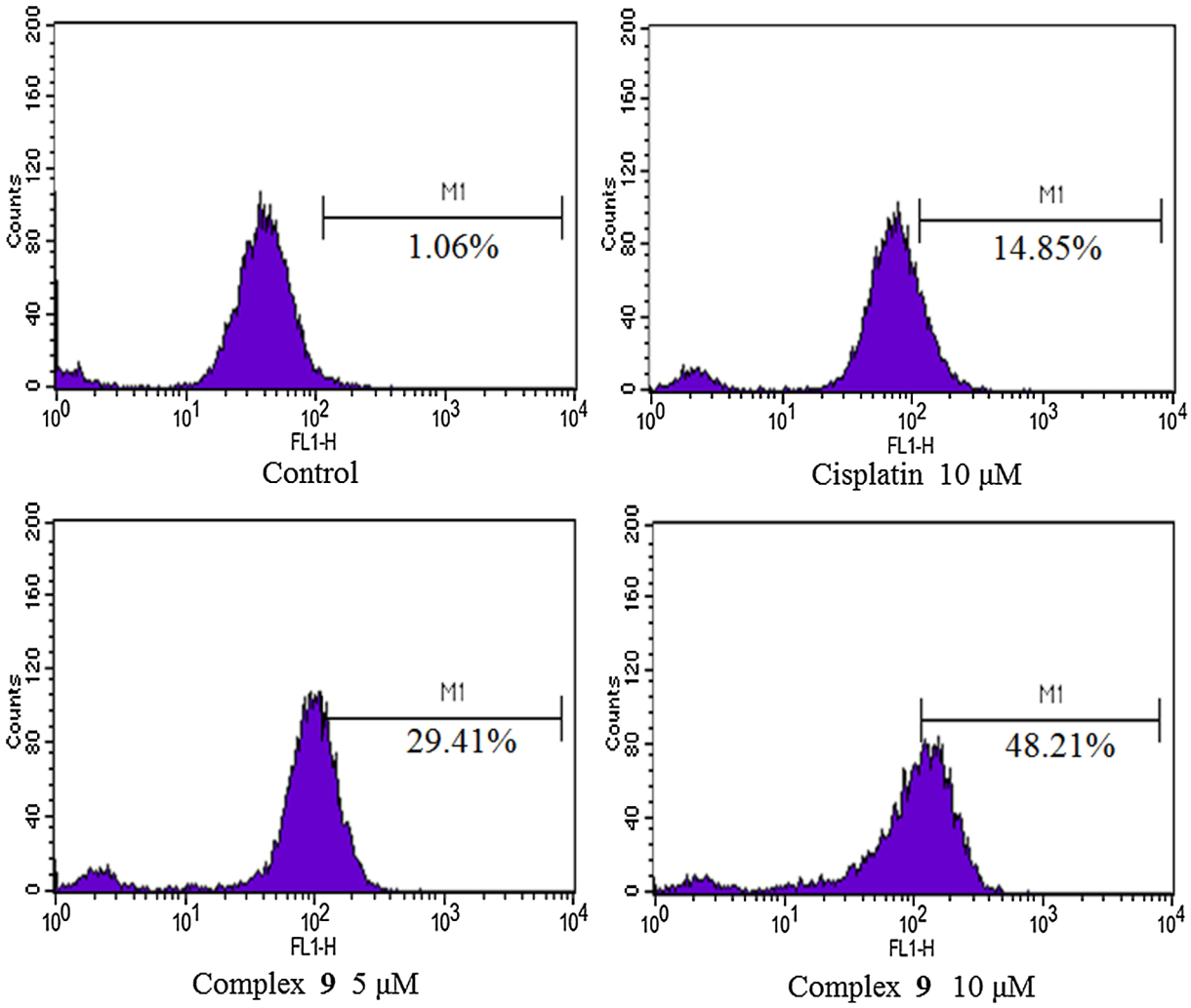

Fig. 9. Intracellular production of ROS by complex **9** and cisplatin following a 24 h incubation using 2′,7′-dichlorodihydrofluorescein diacetate (DCFH-DA) staining analysis by flow cytometry. The experiments were performed three times, and the results of the representative experiments are shown.

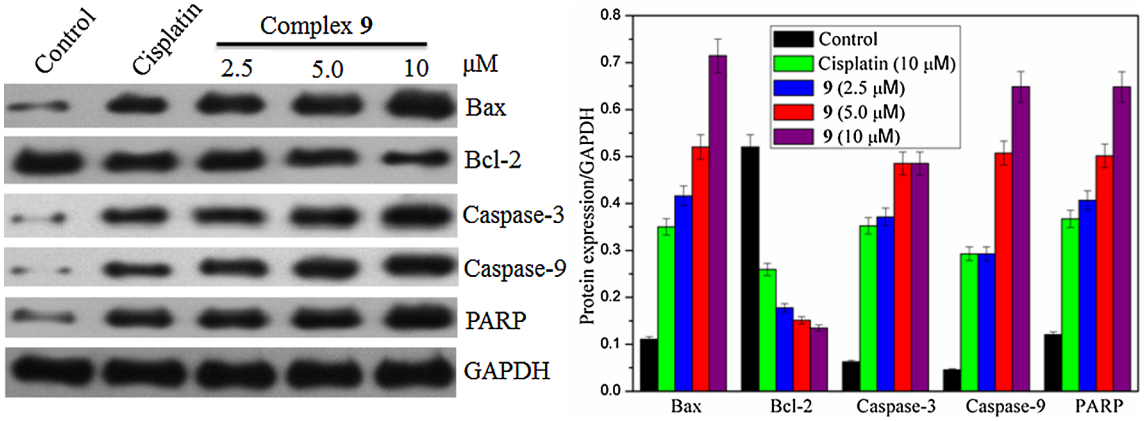

Fig. 10. A549 cells were incubated with complex **9** and cisplatin at the indicated concentrations for 24 h. The expressions of Bax, Bcl-2, caspase-3, caspase-9 and PARP were determined by western blotting assay. GAPDH was used as internal control.

4.4. Cell apoptosis analysis

A549 cells were grown in each well of six-well plates at the density of 0.5×10^5 cells/mL of the RPMI-1640 medium with 10% FBS to the final volume of 2 mL. The A549 cells incubated for overnight in a humidified atmosphere of 5% CO_2 at 37 °C, and then treated with complex **9** (5.0 or 10 μM) and cisplatin (10 μM). After 24 h treatment, the cells were collected, washed thrice in PBS, and re-suspended in 120 μL of binding buffer at a final concentration of 0.5×10^6 cells/mL, and then the cells were incubated with 5 μL of annexin V-FITC and 5 μL of PI in the dark at 4 °C for 30 min. The cells were examined by system software (Cell Quest; BD Biosciences).

4.5. Cell cycle analysis

A549 cells were grown in each well of six-well plates at the density of 0.5×10^5 cells/mL of the RPMI-1640 medium with 10% FBS to the final volume of 2 mL. The A549 cells incubated for overnight in a humidified atmosphere of 5% CO_2 at 37 °C. Then cells treated with complex **9** (5.0 or 10 μM) and cisplatin (10 μM) h in a humidified atmosphere of 5% CO_2 at 37 °C for 24. After 24 h treatment, the cells were collected, washed thrice in PBS, fixed with ice-cold 70% ethanol at −20 °C for overnight. The cells were treated with 100 μg/mL RNase A for 30 min at 37 °C after washed thrice in ice-cold PBS, and finally stained with PI at 1 mg/ml in the dark at 4 °C for 30 min detected by flow cytometry, and the results analysis was performed with the system software (Cell Quest; BD Biosciences).

4.6. Cell migration assay

A wound-healing assay was used to examine the impact of complex **9** on cell migration. A549 cells were seeded in 6-well plates and allowed to grow to ≥95% confluent. After being washed with thrice in PBS, and then wounds were created perpendicular to the lines by 20 μL tips, and unattached cells were removed by washing with thrice in PBS. Then the calcium AM (1 mM stock solution in DMSO with 1:1500 dilution in PBS) was used to stain cells. Cells were washed with thrice in PBS after staining, and then cells treated with complex **9** (5.0 or 10 μM) and cisplatin (10 μM) in a humidified atmosphere of 5% CO_2 at 37 °C for 24. After 24 h treatment, the cells were washed with thrice in PBS, and then photographed to mark the final scratched tracks. The migration rates analyzed by Equation 1: Migration rate (%) = (d1 − d2)/d1. The d1 and d2 represented the width of wound at 0 and 24 h, respectively.

4.7. Transwell migration assay

The cell invasion of A549 cells were evaluated by a transwell migration assay by modified Boyden's chamber in 24-well cell culture plate with a 8 μm pore. Chambers were washed with thrice in PBS and then the medium with the tested compound was placed in the lower chamber, and the A549 cells were seeded in the top chamber. A549 cells were treated with or without complex **9** (5.0 or 10 μM) and cisplatin (10 μM) at 37 °C in a humidified atmosphere of 5% CO_2 for 24 h. After 24 h treatment, the medium was removed and then the cells in the membrane were washed with thrice in PBS. The migrated cells was fixed with 4% paraformaldehyde for 30 min, and stained with 0.2% crystal violet. Images were observed on a fluorescence microscopy.

4.8. Immunofluorescence assay

A549 cells were grown in each well of six-well plates at the density of 0.5×10^5 cells/mL of the RPMI-1640 medium with 10% FBS to the final volume of 2 mL. Cells were treatment with or without complex **9** (5.0 or 10 μM) and cisplatin (10 μM) at 37 °C in a humidified atmosphere of 5% CO_2 for 24 h. After 24 h treatment, cells were fixed with 4% paraformaldehyde at 37 °C for 15 minutes, and then permeabilized with 0.5% Triton X-100/PBS for 15 minutes. After blocking for 30 min in 5% BSA/PBS, cells were washed with PBS and incubated with a-tubulin for 2 h, and then tubulin was immunostained with monoclonal antibody to a-tubulin followed by fluorescence antibody. After the nuclei of cells were labeled with DAPI, and then the cells were visualized by fluorescence microscope.

4.9. Mitochondrial membrane potential (MMP) assay

A549 cells were seeded in six-well plates at the density of 5.0×10^4 cells/mL of the RPMI-1640 medium with 10% FBS to the final volume of 2 mL. The A549 cells were treated with or without complex **9** (5.0 or 10 μM) and cisplatin (10 μM) for 24 h. After 24 h treatment, the A549 cells were then stained with 2 μM JC-1 in the dark at room temperature for 30 min. After 30 min of incubation, the cells were harvested at 2000 rpm and washed thrice in PBS detected using flow cytometry, and the results analysis was performed with the system software (Cell Quest; BD Biosciences).

4.10. Reactive oxygen species (ROS) assay

A549 cells were seeded in six-well plates at the density of 5.0×10^4 cells/mL of the RPMI-1640 medium with 10% FBS to the final volume of 2 mL. The A549 cells were treated with or without complex **9** (5.0 or 10 μM) and cisplatin (10 μM) for 24 h. After 24 h treatment, the A549 cells were then stained with DCFH-DA in the dark at 37 °C for 30 min. After 30 min of incubation, the cells were harvested at 2000 rpm and washed thrice in PBS detected using flow cytometry, and the results analysis was performed with the system software (Cell Quest; BD Biosciences).

4.11. Western blot assay

Western blot analysis was performed as described previously [42,43]. A549 cells were incubated with or without complex **9** (5.0 or 10 μM) and cisplatin (10 μM) for 24 h. After incubation, cells were collected, centrifuged, and washed thrice in PBS. The pellet was then re-suspended in lysis buffer containing 150 mM NaCl, 50 mM Tris (pH 7.4), 1% (w/v) sodium deoxycholate, 1% (v/v) Triton X-100, 0.1% (w/v) SDS, and 1 mM EDTA (Beyotime, China). The lysates were incubated at 37 °C for 30 min, and centrifuged at 20,000g at 4 °C for 10 min. The protein concentration in the supernatant was analyzed by the BCA protein assay reagents. Equal amounts of protein per line were was separated on 12% SDS polyacrylamide gel electrophoresis and transferred to PVDF Hybond-P membrane (GE Healthcare). Membranes were incubated with 5% skim milk in Tris-buffered saline with Tween 20 (TBST) buffer for 1 h and then the membranes being gently rotated overnight at 4 °C. Membranes were then incubated with primary antibodies against Bcl-2, Bax, caspase-3, caspase-9 and PARP or GAPDH for overnight at 4 °C. After three washes in TBST, the membranes were next incubated with peroxidase labeled secondary antibodies for 2 h. Then all membranes were washed with TBST four times for 20 min and the protein blots were detected by chemiluminescence reagent (Thermo Fischer Scientifics Ltd.). The X-ray films were developed with developer and fixed with fixer solution.

Notes

The authors declare no competing financial interest.

Acknowledgments

We are grateful to the National Natural Science Foundation of China (Grant Nos. 21571033, 21977021 and 81760626), and the Ministry of Education Innovation Team Fund (IRT_16R15, 2016GXNSFGA380005), and Natural Science Foundation of Guangxi Province (AB17292075) and Guangxi Funds for Distinguished Experts. We also want to express our gratitude to the New Drug Creation Project of the National Science and Technology Major Foundation of China (Grant No. 2015ZX09101032) for financial aid and the Key University Science Research Project of Jiangsu Province (18KJA360001).

Appendix A. Supplementary material

Supplementary data to this article can be found online at https://doi.org/10.1016/j.bioorg.2019.103236.

References

[1] N.J. Wheate, S. Walker, G.E. Craig, R. Oun, The status of platinum anticancer drugs in the clinic and in clinical trials, Dalton Trans. 39 (2010) 8113–8127.

[2] A. Bergamo, C. Gaiddon, J.H. Schellens, J.H. Beijnen, G. Sava, Approaching tumour therapy beyond platinum drugs: status of the art and perspectives of ruthenium drug candidates, J. Inorg. Biochem. 106 (2012) 90–99.

[3] S.B. Howell, R. Safaei, C.A. Larson, M.J. Sailor, Copper transporters and the cellular pharmacology of the platinum-containing cancer drugs, Mol. Pharmacol. 77 (2010) 887–894.

[4] I. Romero-Canelon, L. Salassa, P.J. Sadler, The contrasting activity of iodido versus chlorido ruthenium and osmium arene Azo- and imino-pyridine anticancer complexes: control of cell selectivity, cross-resistance, p53 dependence, and apoptosis pathway, J. Med. Chem. 56 (2013) 1291–1300.

[5] T.C. Johnstone, K. Suntharalingam, S.J. Lippard, The next generation of platinum drugs: targeted Pt(II) agents, nanoparticle delivery, and Pt(IV) prodrugs, Chem. Rev. 116 (2016) 3436–3486.

[6] K.B. Huang, F.Y. Wang, X.M. Tang, H.W. Feng, Z.F. Chen, Y.C. Liu, Y.N. Liu, H. Liang, Organometallic gold(III) complexes similar to tetrahydroisoquinoline induce ER-stress-mediated apoptosis and pro-death autophagy in A549 cancer cells, J. Med. Chem. 61 (2018) 3478–3490.

[7] W. Liu, R. Gust, Metal N-heterocyclic carbene complexes as potential antitumor metal drugs, Chem. Soc. Rev. 42 (2013) 755–773.

[8] L. Kelland, The resurgence of platinum-based cancer chemotherapy, Nat. Rev. Cancer 7 (2007) 573–584.

[9] J. Ma, Q.P. Wang, Z.L. Huang, X.D. Yang, Q.D. Nie, W.P. Hao, P.G. Wang, X. Wang, Glycosylated platinum(IV) complexes as substrates for glucose transporters (GLUTs) and organic cation transporters (OCTs) exhibited cancer targeting and human serum albumin binding properties for drug delivery, J. Med. Chem. 60 (2017) 5736–5748.

[10] L.L. Ma, R. Ma, Y.P. Wang, X.Y. Zhu, J.L. Zhang, H.C. Chan, X.F. Chen, W.J. Zhang, S.K. Chiu, G.Y. Zhu, Chalcoplatin, a dual-targeting and p53 activator containing anticancer platinum(IV) pro-drug with unique mode of action, Chem. Commun. 51 (2015) 6301–6304.

[11] X.P. Han, S. Jin, Y.J. Wang, Z.G. He, Recent advances in platinum(IV) complex based delivery systems to improve platinum(II) anticancer therapy, Med. Res. Rev. 35 (2015) 1268–1299.

[12] M. Fanelli, M. Formica, V. Fusi, L. Giorgi, M. Micheloni, P. Paoli, New trends in platinum and palladium complexes as antineoplastic agents, Coordin. Chem. Rev. 310 (2016) 41–79.

[13] R.K. Pathak, S. Marrache, J.H. Choi, T.B. Berding, S. Dhar, The Pro-drug platin-A: simultaneous release of cisplatin and aspirin, Angew. Chem. Int. Ed. 53 (2014) 1963–1967.

[14] X.D. Qin, L. Fang, F.H. Chen, S.H. Gou, Conjugation of platinum(IV) complexes with chlorambucil to overcome cisplatin resistance via a “joint action” mode toward DNA, Eur. J. Med. Chem. 137 (2017) 167–175.

[15] R. Raveendran, J.P. Braude, E. Wexselblatt, V. Novohradsky, O. Stuchlikova, V. Brabec, V. Gandin, D. Gibson, Pt(IV) Derivatives of cisplatin and oxaliplatin with phenylbutyrate axial ligands are potent cytotoxic agents that act by several mechanisms of action, Chem. Sci. 7 (2016) 2381–2391.

[16] F.H. Chen, X.C. Huang, M. Wu, S.H. Gou, W.W. Hu, A CK2-targeted Pt(IV) prodrug to disrupt DNA damage response, Canc. Lett. 385 (2017) 168–178.

[17] J. Shi, P.W. Kantoff, R. Wooster, O.C. Farokhzad, Cancer nanomedicine: progress, challenges and opportunities, Nat. Rev. Cancer 17 (2016) 20–37.

[18] Y. Li, J.Y. Lin, J.Y. Ma, L. Song, H.R. Lin, B.W. Tang, D.Y. Chen, G.H. Su, S.F. Ye, X. Zhu, F.H. Luo, Z.Q. Hou, Methotrexate-camptothecin prodrug nanoassemblies as a versatile nanoplatform for biomodal imaging-guided self-active targeted and synergistic chemotherapy, ACS Appl. Mater. Interf. 9 (2017) 34650–34665.

[19] P. Huang, D.L. Wang, Y. Su, W. Huang†, Y.F. Zhou, D.X. Cui, X.Y. Zhu, D.Y. Yan, Combination of small molecule prodrug and nanodrug delivery: amphiphilic drug-drug conjugate for cancer therapy, J. Am. Chem. Soc. 136 (2014) 11748–11756.

[20] G.R. Pettit, S.B. Singh, E. Hamel, C.M. Lin, D.S. Alberts, D. Garcia-Kendall, Isolation and structure of the strong cell growth and tubulin inhibitor combretastatin A-4, Experientia 45 (1989) 209–211.

[21] R.P. George, M.R. Rhodes, D.L. Herald, E. Hamel, J.M. Schmidt, R.K. Pettit, Antineoplastic agents. 445. Synthesis and evaluation of structural modifications of (Z)- and (E)-combretastatin A-4, J. Med. Chem. 48 (2005) 4087–4099.

[22] P. Suman, T.R. Murthy, K. Rajkumar, D. Srikanth, C. Dayakar, C. Kishor, A. Addlagatta, S.V. Kalivendi, B.C. Raju, Synthesis and structureeactivity relationships of pyridinyl-1H-1,2,3-triazolyldihydroisoxazoles as potent inhibitors of tubulin polymerization, Eur. J. Med. Chem. 90 (2015) 603–619.

[23] R. Wu, W.J. Ding, T. Liu, H. Zhu, Y.Z. Hu, B. Yang, Q.J. He, XN05, a novel synthesized microtubule inhibitor, exhibits potent activity against human carcinoma cells *in vitro*, Canc. Lett. 285 (2009) 13–22.

[24] H. Chen, Y.M. Li, C.Q. Sheng, Z.L. Lv, G.Q. Dong, T.T. Wang, J. Liu, M.F. Zhang, L.Z. Li, T. Zhang, D.P. Geng, C.J. Niu, K. Li, Design and synthesis of cyclopropylamide analogues of combretastatin – a 4 as novel microtubule-stabilizing agents, J. Med. Chem. 56 (2013) 685–699.

[25] V. Chaudhary, J.B. Venghateri, H.P. Dhaked, A.S. Bhoyar, S.K. Guchhait, D. Panda, Novel combretastatin-2-aminoimidazole analogues as potent tubulin assembly Inhibitors: exploration of unique pharmacophoric impact of bridging skeleton and aryl moiety, J. Med. Chem. 59 (2016) 3439–3451.

[26] G.R. Pettit, G.M. Cragg, D.L. Herald, J.M. Schmidt, P. Lohavanijaya, Isolation and structure of combretastatin, Can. J. Chem. 60 (1982) 1374–1376.

[27] A. Kamal, A. Mallareddy, M.J. Ramaiah, S. Pushpavalli, P. Suresh, C. Kishor, J. Murty, N.S. Rao, S. Ghosh, A. Addlagatta, M. Pal-Bhadra, Synthesis and biological evaluation of combretastatin-amidobenzothiazole conjugates as potential anticancer agents, Eur. J. Med. Chem. 56 (2012) 166–178.

[28] G.R. Pettit, Matthew P. Grealish, M. Katherine Jung, Ernest Hamel, Robin K. Pettit, J.C. Chapuis, J.M. Schmidt, Antineoplastic agents. 465. Structural modification of resveratrol: sodium resverastatin phosphate[1], J. Med. Chem. 45 (2002) 2534–2542.

[29] G.R. Pettit, S.B. Singh, M.R. Boyd, E. Hamel, R.K. Pettit, J.M. Schmidt, F. Hogan, Antineoplastic agents. 291. Isolation and synthesis of combretastatins A-4, A-5, and A-6[1a], J. Med. Chem. 38 (1995) 1666–1672.

[30] M. Ravera, E. Gabano, G. Pelosi, F. Fregonese, S. Tinello, D. Osella, A new entry to asymmetric platinum(IV) complexes via oxidative chlorination, Inorg. Chem. 53 (2014) 9326–9335.

[31] L.L. Ma, R. Ma, Z.G. Wang, S.M. Yiu, G.Y. Zhu, Heterodinuclear Pt(IV)-Ru(II) anticancer prodrugs to combat both drug resistance and tumor metastasis, Chem. Commun. 52 (2016) 10735–10738.

[32] J.J. Chen, J.X. Ding, W.G. Xu, T.M. Sun, H.H. Xiao, X.L. Zhuang, X.S. Chen, Receptor and microenvironment dual-recognizable nanogel for targeted chemotherapy of highly metastatic malignancy, Nano Lett. 17 (2017) 4526–4533.

[33] M.A. Jordan, L. Wilson, Microtubules as a target for anticancer drugs, Nat. Rev. Cancer 4 (2004) 253–265.

[34] M. Kavallaris, Microtubules and resistance to tubulin binding agents, Nat. Rev. Cancer 10 (2010) 194–204.

[35] Y. Li, C.P. Tan, W. Zhang, L. He, L.N. Ji, Z.W. Mao, Phosphorescent iridium(III)-bis-N-heterocyclic carbene complexes as mitochondria-targeted theranostic and photodynamic anticancer agents, Biomaterials 39 (2015) 95–104.

[36] S. Wen, D. Zhu, P. Huang, Targeting cancer cell mitochondria as a therapeutic approach, Future Med. Chem. 5 (2013) 53–67.

[37] R.M. Hughes, D.J. Freeman, K.N. Lamb, R.M. Pollet, W.J. Smith, D.S. Lawrence, Optogenetic apoptosis: light-triggered cell death, Angew. Chem., Int. Ed. 54 (2015) 12064–12068.

[38] M.P. Murphy, How mitochondria produce reactive oxygen species, Biochem. J. 417 (2009) 1–13.

[39] H.U. Simon, A. Haj-Yehia, F. Levi-Schaffer, Role of reactive oxygen species (ROS) in apoptosis induction, Apoptosis 5 (2000) 415–418.

[40] S.H. Huang, L.W. Wu, A.C. Huang, C.C. Yu, J.C. Lien, Y.P. Huang, J.S. Yang, J.H. Yang, Y.P. Hsiao, W.G. Wood, C.S. Yu, J.G. Chung, Benzyl isothiocyanate (BITC) induces G2/M phase arrest and apoptosis in human melanoma A375.S2 cells through reactive oxygen species (ROS) and both mitochondria-dependent and death receptor-mediated multiple signaling pathways, J. Agric. Food Chem. 60 (2012) 665–675.

[41] J. Wang, J. Yi, Cancer cell killing via ROS: to increase or decrease, that is the question, Cancer Biol. Ther. 7 (2008) 1875–1884.

[42] S.H. Huang, L.W. Wu, A.C. Huang, C.C. Yu, J.C. Lien, Y.P. Huang, J.S. Yang, J.H. Yang, Y.P. Hsiao, W.G. Wood, C.S. Yu, J.G. Chung, Benzyl isothiocyanate BITC) induces G2/M phase arrest and apoptosis in human melanoma A375.S2 cells through reactive oxygen species (ROS) and both mitochondria dependent and death receptor-mediated multiple signaling pathways, J. Agric. Food Chem. 60 (2012) 665–675.

[43] J. Yan, J. Chen, S. Zhang, J.H. Hu, L. Huang, X.S. Li, Synthesis, evaluation, and mechanism study of novel indole-chalcone derivatives exerting effective antitumor activity through microtubule destabilization *in vitro* and *in vivo*, J. Med. Chem. 59 (2016) 5264–5283.